Tissue-specific expression of Cre recombinase from theTgfb3 locus

ARTICLE *in* GENESIS · FEBRUARY 2008

Impact Factor: 2.02 · DOI: 10.1002/dvg.20372 · Source: PubMed

Liang-Tung Yang
National Health Research Institutes

Wai-Yee li
University of British Columbia - Vancouver

Published in final edited form as:
Genesis. 2008 February ; 46(2): 112–118.

Tissue-specific expression of Cre recombinase from the *Tgfb3* locus

Liang-Tung Yang, **Wai-Yee Li**, and **Vesa Kaartinen***
Developmental Biology Program, The Saban Research Institute of Childrens Hospital Los Angeles, Departments of Pathology and Surgery, Keck School of Medicine, University of Southern California, Los Angeles, CA 90027, USA

Summary

Tgfb3, a member of the TGF-β superfamily, is tightly regulated, both spatially and temporally, during embryogenesis. Previous mouse knockout studies have demonstrated that *Tgfb3* is absolutely required for normal palatal fusion and pulmonary development. We have generated a novel tool to ablate genes in *Tgfb3*-expressing cells by targeting the promoterless *Cre-pgk-Neo* cassette into exon 1 of the mouse *Tgfb3* gene, which generates a functionally null *Tgfb3* allele. Using the Rosa26 reporter assay, we demonstrate that *Cre*-induced recombination was already induced at embryonal day 10 (E10) in the ventricular myocardium, limb buds and otic vesicles. At E14, robust recombination was detected in the prefusion palatal epithelium. Deletion of the TGF-β type I receptor *Alk5* (*Tgfbr1)* specifically in *Tgfb3* expressing cells using the *Tgfb3-Cre* driver line lead to a cleft palate phenotype similar to that seen in conventional *Tgfb3* null mutants. In addition, *Alk5/Tgfb3-Cre* mice displayed hydrocephalus, and severe intracranial bleeding due to germinal matrix hemorrhage.

Keywords

TGF-β; palatogenesis; cleft palate; Transforming growth factor; development; mouse

In mammals, three different TGF-β-isoforms (TGF-β1, -β2 and –β3) are encoded by three separate genes. Their expression patterns are both spatially and temporally distinct during embryogenesis, and knockout studies have demonstrated that they display specialized roles *in vivo* (Shull et al. 1992;Proetzel et al. 1995;Kaartinen et al. 1995;Sanford et al. 1997). Mice lacking *Tgfb3* display a specific non-redundant role in palatal fusion, which is consistent with its strong and specific expression in the epithelium of the prefusion palatal shelves. Subsequent studies have shown that during palatogenesis TGF-β3 regulates adhesion and intercalation of midline epithelial cells, programmed cell death, and degradation of the basement membrane (Blavier et al. 2001;Cuervo et al. 2002;Martinez-Alvarez et al. 2000;Gato et al. 2002).

TGF-βs signal through functional heterotetrameric complexes that contain two type II (*Tgfbr2*) and two type I (*Alk5*) transmembrane serine/threonine kinase receptors (Derynck and Feng 1997;Massague 1998). Deletion of *Alk5* and *Tgfbr2* in the palatal epithelium using the cytokeratin-14 (K14) promoter-driven Cre recombinase has demonstrated the importance of these two genes in palatal fusion (Dudas et al. 2006;Xu et al. 2006). Although cytokeratin promoter regions, e.g., K5 and K14, are valuable for targeting transgene expression to epithelia with different differentiation states, none of the existing keratin promoters can mimic the spatio-temporal expression of *Tgfb3* during palatogenesis.

*Corresponding author: vkaartinen@chla.usc.edu.

To provide a tool to study genes involved in palatal fusion and other developmental processes controlled by TGF-β3, we generated a *Tgfb3*-Cre knockin mouse model (Fig. 1). This was achieved by replacing the coding region of the *Tgfb3* gene with the promoterless *Cre-pgkneo* cassette. Since all the promoter and regulatory elements of the *Tgfb3* gene were essentially preserved, we predicted that *Cre* expression would faithfully recapitulate the endogenous expression pattern of the *Tgfb3* gene. Once the heterozygote mice carrying the *Cre-PGK-Neo* cassette in the *Tgfb*3 locus were obtained, we analyzed *Tgfb3-Cre*-induced recombination during embryogenesis using the ROSA26R reporter assay (Soriano 1999). Cre-induced lacZ expression was examined by X-gal staining of the *Tgfb3*-Cre;R26R embryos from timed pregnancies in order to confirm the correlation between tissue-specific Cre activity and the previously published *Tgfb3* expression pattern detected by *in situ* hybridization (Pelton et al. 1990;Millan et al. 1991). Moreover, in this analysis, β-galactosidase expression also marks cells that have expressed *Tgfb3* at any earlier developmental time point.

Using whole mount lacZ staining, we observed the earliest β-galactosidase activity around embryonal day 8 (6–8 somite pairs) when a few scattered positively-staining cells became detectable (Fig. 2A, inset). At E9 (~16 somite pairs), β-galactosidase staining could be seen in the heart, pharyngeal arches and otic vesicle (Fig. 2B). At E10.0, scattered staining was observed in the ectoderm including the pharyngeal arches and limb buds. Strong *lacZ* staining was also detected in the otic vesicles, mid-brain, heart, somites, and tail (Fig. 2D, E). By E11, positive staining was more apparent at the pharyngeal arches and somatic regions. The left ventricle also stained strongly positive for *lacZ* (Fig. 2F, G). Sagittal sections of the X-gal stained embryos revealed that primodia of the mid-brain and hindbrain were *LacZ*-positive (Fig. 3A). At E14.0, the Cre-induced recombination was strikingly strong in the palatal epithelium (Fig. 2 I, L, M), while some sporadic positively staining cells could also be seen in the palatal mesenchyme (Fig. 2L, M). Positive staining was also detectable in the whisker follicles (Fig. 2H, J) and in the cartilaginous structures of the developing limbs (Fig. 2H), as well as in many mesenchymal structures in the lower jaw and the tongue (Fig. 2N). In contrast to the K14 expression pattern, which was restricted to relatively undifferentiated basal keratinocytes of the epidermis, transverse sections of the skin at E14 showed punctate staining in the epidermis (Fig. 2K). Coronal sections through the head showed positive staining in the choroid plexus of the IVth ventricle and lateral ventricles (Fig. 3B, C), as well as in the nasal epithelium (Fig. 3F). Sagittal sections through the head showed positive staining in vascular structures of the germinal matrix (Fig. 3 D, E). To summarize, *lacZ* positive staining of the palatal epithelium, the nasal epithelium, and the epithelium of the choroid plexus recapitulate the expression pattern previously reported for *Tgfb3* via *in situ* hybridization (Pelton et al. 1990;Fitzpatrick et al. 1990;Millan et al. 1991). The expression of *Tgfb3* in the vessel-like structures of the germinal matrix is previously unreported, indicating that TGFβ signaling may play a role in germinal matrix development.

To test whether the *Tgfb3*-Cre allele can induce efficient recombination in the palatal epithelium, we crossed male mice heterozygous for the *Tgfb3-Cre* and *Alk5* knockout alleles with female mice homozygous for the *floxed Alk5* allele (Larsson et al. 2001). Specific ablation of the *Alk5* gene in *Tgfb3*-expressing cells, including the palatal epithelium, should theoretically lead to a cleft palate phenotype, since TGF-β3 knockout mice display complete cleft palate (Kaartinen et al. 1995;Proetzel et al. 1995). Embryos were harvested at E17.0 and the palatal phenotype was analyzed using stereomicroscopic and histological analyses (Fig. 4). Indeed, $Alk5^{KO/FX}$/$Tgfb3\text{-}Cre^{HE}$ (termed herein *Alk5/Tgfb3-Cre)* mice displayed a complete cleft of the secondary palate identical to that seen in *Tgfb3* knockout mice. This result demonstrated that *Tgfb3*-Cre mice can be used as a tool to assess the function of genes in the palatal epithelium during palate formation.

In addition to cleft palate, at E17 *Alk5/Tgfb3-Cre* mice displayed intracranial hemorrhage and tissue destruction at the hindbrain region (Fig. 5 A-F). Coronal sections of the brain revealed that mutant mice suffer from hydrocephalus, with pronounced dilatation of all the ventricles. Pressure generated from the increased volume of cerebrospinal fluid (CSF) led to compression of the cerebellum. Subsequent studies indicated that the intracranial bleeding was already detectable in embryos at E14 stage. We excluded the cause of this bleeding being secondary to incompetence of the major arteries of the brain by injection of Indian ink to the left cardiac ventricle at E14 (Fig. 5 G, H). Instead, detailed analysis of this intracranial bleeding revealed a blood clot that was trapped in the region surrounding the venous sinuses (Fig. 5I), the site where CSF is absorbed into the venous system. This observation, together with the finding that all ventricles were dilated and the neural tube was not completely closed at E17, suggest that deletion of *Alk5* in the TGF-β3 expressing cells caused a non-obstructive type of hydrocephalus with blood clotting at the CSF absorption area, possibly the arachnoid villi. Moreover, histological analysis of sagittal sections of the mutant head at E14 demonstrated bleeding in the germinal matrix, resulting in intraventricular bleeding (Fig. 5J-O). These results imply a role for TGFβ signaling in maintenance of vasculature integrity within the germinal matrix. Therefore, the *Tgfb3*-Cre mouse also provides a powerful tool for studies of the blood-brain barrier.

To conclude, the *Tgfb3-Cre* mouse model will be a valuable tool to analyze genes of interest in the prefusion palatal epithelium during facial development. We expect that in these mice, temporal control of Cre expression will be more accurately achieved than in *K14-Cre* mice, which have been traditionally used to induce recombination in the palatal epithelium (Gritli-Linde 2007;Wang et al. 2006;Xu et al. 2006). Moreover, these mice may be used to assess gene function in other organs and cell types, including vasculature of the central nervous system.

Material and Methods

Generation of the *Tgfb3*-Cre mouse line

A targeting vector was generated by combining a 9-kb clone isolated from the B6xCBA (F1) mouse genomic library (right arm), a 1.6-kb PCR fragment amplified from the R1-ES cell DNA (left arm), and a cassette containing a promoterless Cre gene and a neomycin-resistant gene driven by the phosphoglycerate kinase promoter (PGK-Neo) to replace the coding region of the ATG containing exon 1 of the *Tgfb3* gene. Briefly, a 1.6-kb PCR-amplified 5′ XbaI-BamHI genomic fragment, the Cre-pgk-Neo, and a 10-kb 3′ NotI-EcoRI genomic fragment (generated by fusing a 2.6-kb Not1-Kpn1 PCR fragment with a 7.6-kb KpnI-EcoRI fragment from the library clone) containing exons 2 and 3 were subcloned into the pKOdt plasmid (Stratagene). R1-ES cells were cultured, electroporated and screened as previously described (Kaartinen et al., 1995; Kaartinen et al., 2004). Targeted colonies were initially identified by PCR amplification of a 2-kb fragment using a 5′-arm outside sense primer, primer1 (GCATGCTCCAGACTGCCTTGGGA) and a Cre anti-sense primer, primer 2 (CCTCATTCACTCGTTGCATCGACCGG). Southern blot analyses of genomic DNAs, digested with both ClaI and KpnI, were used to confirm homologous recombination of the targeted allele using the Cre and Neo probes. A total of 7 positive homologous recombinant ES cells clones were obtained from 260 G418-resistant clones. ES cells from two independent targeted clones were microinjected into C57/BL6J blastocysts by the transgenic core facility at the University of Southern California. Three male chimeras (male/female ratio was 9:3) were used to produce heterozygote *Tgfb3-Cre* mice.

Mouse breeding, embryo isolation, and genotype assays

ROSA26 Cre reporter mice were obtained from the Jackson laboratory (Bar Harbor, ME, USA). Mice carrying the Alk5^{flox} and Alk5^{ko} alleles were obtained from S. Karlsson (Lund University

Hospital, Lund, Sweden). *Tgfb3*-Cre mice were generated as described above. All mice were bred to have a mixed genetic background. Mice were mated during the dark period of the controlled light cycle. Female mice acquiring vaginal plugs were designated as day 0. At the time interval indicated in respective figures (E14 to E17), females were euthanized by CO_2 and embryos were extracted in PBS (Invitrogen) followed by further analyses. All studies and procedures performed on mice were carried out at the Animal Care Facility of the Saban Research Institute, and were approved by the CHLA Animal Care and Use Committee (IACUC). Mouse tail biopsies were colleted and genotyped by PCR. Oligos for genotyping of the $Alk5^{flox,}$ $Alk5^{ko}$, and Cre alleles have been described elsewhere (Dudas et al. 2006).

Histological analyses and X-gal staining

Mouse embryos or tissues were fixed in 4% formaldehyde plus 0.2% glutaraldehyde for 24 h, and paraffin sections were stained with hematoxylin-eosin following the standard procedure. For whole-mount X-gal staining, embryos or tissues were fixed in 2% formaldehyde plus 0.2% glutaraldehyde for 20 minutes at RT, washed in a detergent wash solution, and developed in X-gal solution for 4 hours to overnight. For X-gal staining of frozen sections, tissues were fixed in 4% formaldehyde for 30 minutes on ice, and embedded in OCT. Frozen sections were then stained with X-gal solution for 5 hours (Hogan et al., 1994).

Acknowledgements

We thank S. Karlsson for the $Alk5^{FXFX}$ mice and I. Gonzalez-Gomez for help in phenotype analyses. LTY was supported by a grant from the CIRM (T2-00005) and VK by grants from the NIH (HL074862 and DE013085).

Reference List

Blavier L, Lazaryev A, Groffen J, Heisterkamp N, DeClerck YA, Kaartinen V. TGF-beta3-induced palatogenesis requires matrix metalloproteinases. Mol Biol Cell 2001;12:1457–1466. [PubMed: 11359935]

Cuervo R, Valencia C, Chandraratna RA, Covarrubias L. Programmed cell death is required for palate shelf fusion and is regulated by retinoic acid. Dev Biol 2002;245:145–156. [PubMed: 11969262]

Derynck R, Feng XH. TGF-beta receptor signaling. Biochim Biophys Acta 1997;1333:F105–F150. [PubMed: 9395284]

Dudas M, Kim J, Li WY, Nagy A, Larsson J, Karlsson S, Chai Y, Kaartinen V. Epithelial and ectomesenchymal role of the type I TGF-beta receptor ALK5 during facial morphogenesis and palatal fusion. Dev Biol 2006;296:298–314. [PubMed: 16806156]

Fitzpatrick DR, Denhez F, Kondaiah P, Akhurst RJ. Differential expression of TGF beta isoforms in murine palatogenesis. Development 1990;109:585–595. [PubMed: 2401212]

Gato A, Martinez ML, Tudela C, Alonso I, Moro JA, Formoso MA, Ferguson MW, Martinez-Alvarez C. TGF-beta(3)-induced chondroitin sulphate proteoglycan mediates palatal shelf adhesion. Dev Biol 2002;250:393–405. [PubMed: 12376112]

Gritli-Linde A. Molecular control of secondary palate development. Dev Biol 2007;301:309–326. [PubMed: 16942766]

Kaartinen V, Voncken JW, Shuler C, Warburton D, Bu D, Heisterkamp N, Groffen J. Abnormal lung development and cleft palate in mice lacking TGF-beta 3 indicates defects of epithelial-mesenchymal interaction. Nat Genet 1995;11:415–421. [PubMed: 7493022]

Larsson J, Goumans MJ, Sjostrand LJ, van Rooijen MA, Ward D, Leveen P, Xu X, ten Dijke P, Mummery CL, Karlsson S. Abnormal angiogenesis but intact hematopoietic potential in TGF-beta type I receptor-deficient mice. EMBO J 2001;20:1663–1673. [PubMed: 11285230]

Martinez-Alvarez C, Bonelli R, Tudela C, Gato A, Mena J, O'Kane S, Ferguson MW. Bulging medial edge epithelial cells and palatal fusion. Int J Dev Biol 2000;44:331–335. [PubMed: 10853831]

Massague J. TGF-beta signal transduction. Annu Rev Biochem 1998;67:753–791. [PubMed: 9759503]

Millan FA, Denhez F, Kondaiah P, Akhurst RJ. Embryonic gene expression patterns of TGF beta 1, beta 2 and beta 3 suggest different developmental functions in vivo. Development 1991;111:131–143. [PubMed: 1707784]

Pelton RW, Dickinson ME, Moses HL, Hogan BL. In situ hybridization analysis of TGF beta 3 RNA expression during mouse development: comparative studies with TGF beta 1 and beta 2. Development 1990;110:609–620. [PubMed: 1723948]

Proetzel G, Pawlowski SA, Wiles MV, Yin M, Boivin GP, Howles PN, Ding J, Ferguson MW, Doetschman T. Transforming growth factor-beta 3 is required for secondary palate fusion. Nat Genet 1995;11:409–414. [PubMed: 7493021]

Sanford LP, Ormsby I, Gittenberger-de Groot AC, Sariola H, Friedman R, Boivin GP, Cardell EL, Doetschman T. TGFbeta2 knockout mice have multiple developmental defects that are non-overlapping with other TGFbeta knockout phenotypes. Development 1997;124:2659–2670. [PubMed: 9217007]

Shull MM, Ormsby I, Kier AB, Pawlowski S, Diebold RJ, Yin M, Allen R, Sidman C, Proetzel G, Calvin D. Targeted disruption of the mouse transforming growth factor-beta 1 gene results in multifocal inflammatory disease. Nature 1992;359:693–699. [PubMed: 1436033]

Soriano P. Generalized lacZ expression with the ROSA26 Cre reporter strain. Nat Genet 1999;21:70–71. [PubMed: 9916792]

Wang J, Nagy A, Larsson J, Dudas M, Sucov HM, Kaartinen V. Defective ALK5 signaling in the neural crest leads to increased postmigratory neural crest cell apoptosis and severe outflow tract defects. BMC Dev Biol 2006;6:51–51. [PubMed: 17078885]

Xu X, Han J, Ito Y, Bringas P Jr, Urata MM, Chai Y. Cell autonomous requirement for Tgfbr2 in the disappearance of medial edge epithelium during palatal fusion. Dev Biol 2006;297:238–248. [PubMed: 16780827]

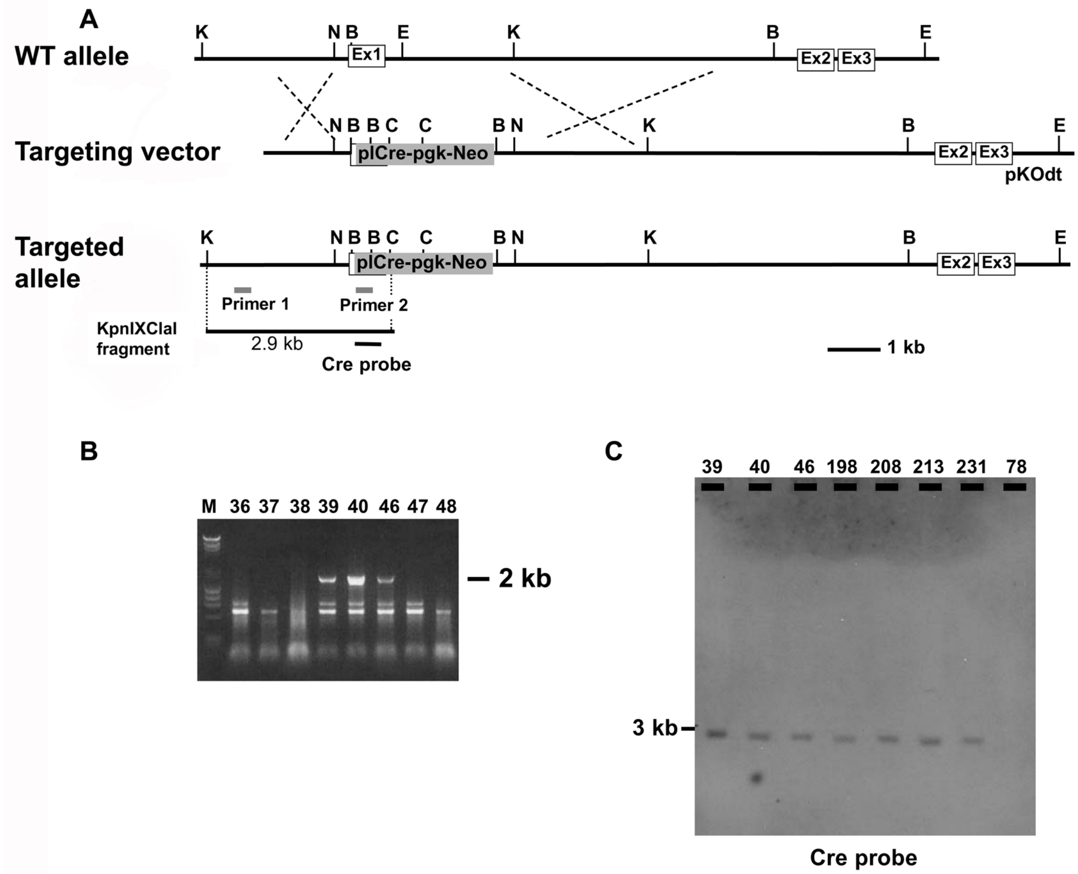

FIG. 1.

Generation of *Tgfb3-Cre* mice. (a) A schematic diagram of the *Tgfb3-Cre* targeting construct and the strategy for identifying the tar- geted allele. Gray shaded *pl Cre/Neo* box: the promotorless *Cre* gene followed by the neomycin-resistant gene driven by a *pgk* promoter; Ex1, Ex2, Ex3: Exon1, Exon2, and Exon3; K: *Kpn*I, X: *Xho*I, B: *BamH*I, E: *Eco*RI, C: *Cla*I, N: *Not*I. (b) PCR-screening using primers 1 and 2 generated a 2-kb amplification product when DNA from correctly targeted clones (39, 40, 46) was used as a template. (c) Southern blot analysis of the targeted ES clones identified by PCR screening. Genomic DNAs from seven PCR-positive ES clones were doubly digested with Cla I and Kpn I, and probed with the Cre probe. The Cre probe identified a 2.9-kb band for the targeted allele.

NIH-PA Author Manuscript

NIH-PA Author Manuscript

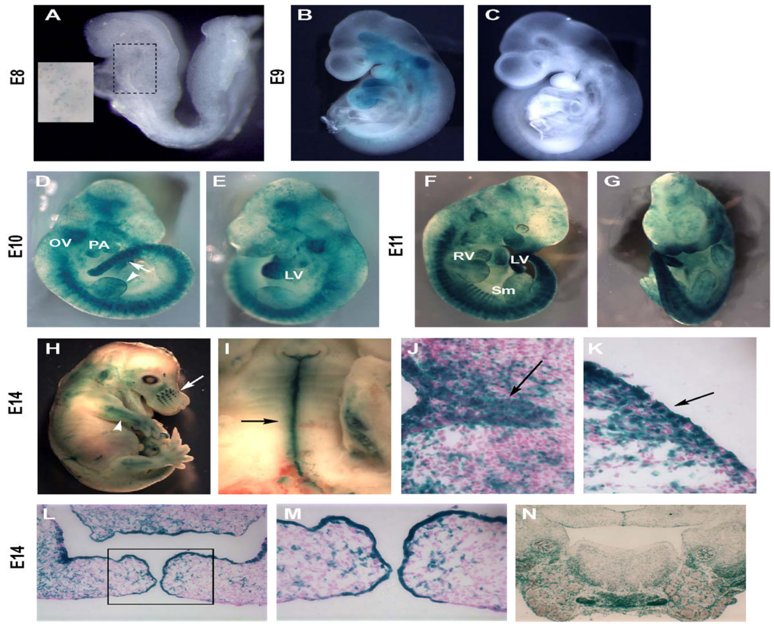

FIG. 2.

Analysis of the *Tgfb3* expression pattern by *Cre*-induced recombination in *Rosa26* reporter (R26R) mice. Embryos from timed matings between the *R26R* and the *Tgfb3-Cre* mice were stained with X-gal to follow *Tgfb3* expressing cell lineages (a–g). Positive *X-gal* staining becomes visible at E8 (a, 6–8 somite pairs) (high power image shown in the inset). At E9, positive staining can be seen in the heart, pharyngeal arches and otic vesicle (b, 16 somite pairs). *Cre*-negative littermate did not demonstrate any detectable β-galactosidase activity (c). Whole-mount X-gal staining at E10 shows a positive staining in regions of the midbrain, otic vesicle (OV), somites, paryngeal arches (PA), left ventricle (LV), limb buds (arrow head), and the tail (arrow) (d,e). Whole-mount *X-gal* staining at E11 reveals positive staining in the LV, right ventricle (RV), and particularly in somites (Sm) (f,g). Whole-mount *X-gal* staining at E14. Positive staining can be seen in the whisker follicles (h, arrow), cartilaginous structures of the limbs (h, arrowhead), and the midline palatal epithelium (i, arrow). (j–n) Transverse sections of the head at E14 stained with *X-gal*. The whisker follicle (j), the skin (k), the palatal epithelium (l, m), and many mesenchymal structures of the lower jaw and the tongue (n) stained positive for *lacZ*. (m) is a higher magnification of the boxed region in (l).

NIH-PA Author Manuscript
NIH-PA Author Manuscript

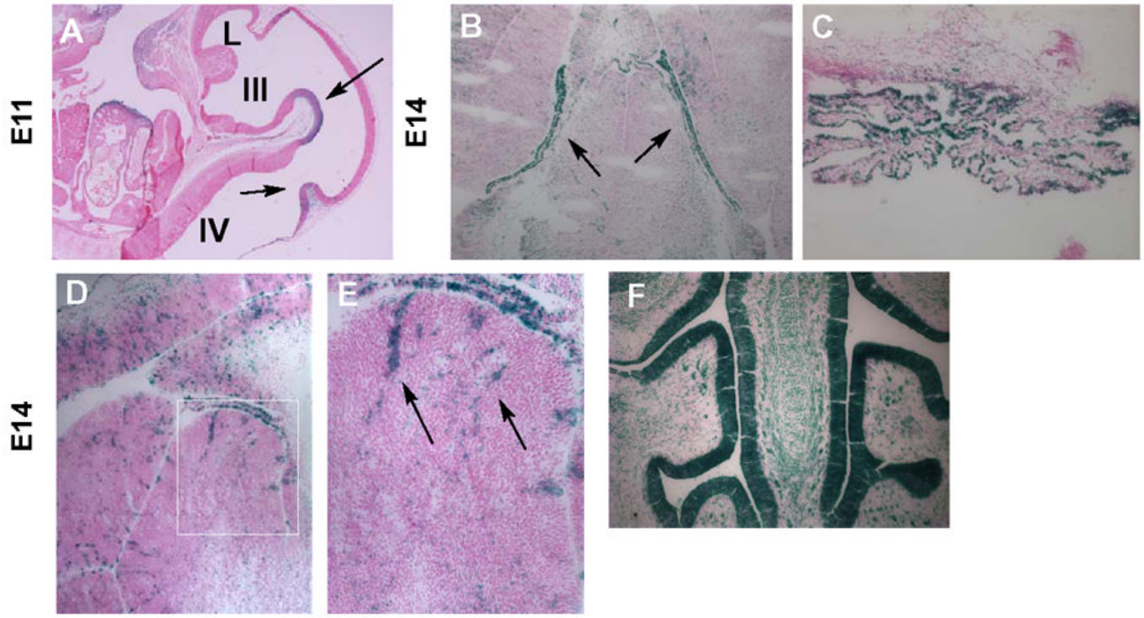

FIG. 3.

Tgfb3-Cre-induced recombination in *Rosa26* reporter (R26R) mice. (a) Sagittal sections of the *X-gal*-stained embryos at E11 show positive staining in the primodia of midbrain and hindbrain (arrows). L: lateral ventricle; III: third ventricle; IV: fourth ventricle. (b,c,f) Coronal sections of the head at E14 stained with *X-gal* displayed positive staining in the epithelial layer of choroid plexus of the lateral ventricles (b, arrow) and IVth ventricle (c), and the nasal epithelium (f). (d,e) Sagittal sections of the head at E14 stained with X-gal showed positive staining in vascular structures of the germinal matrix (arrows). (e) is a higher magnification of the boxed region in (d).

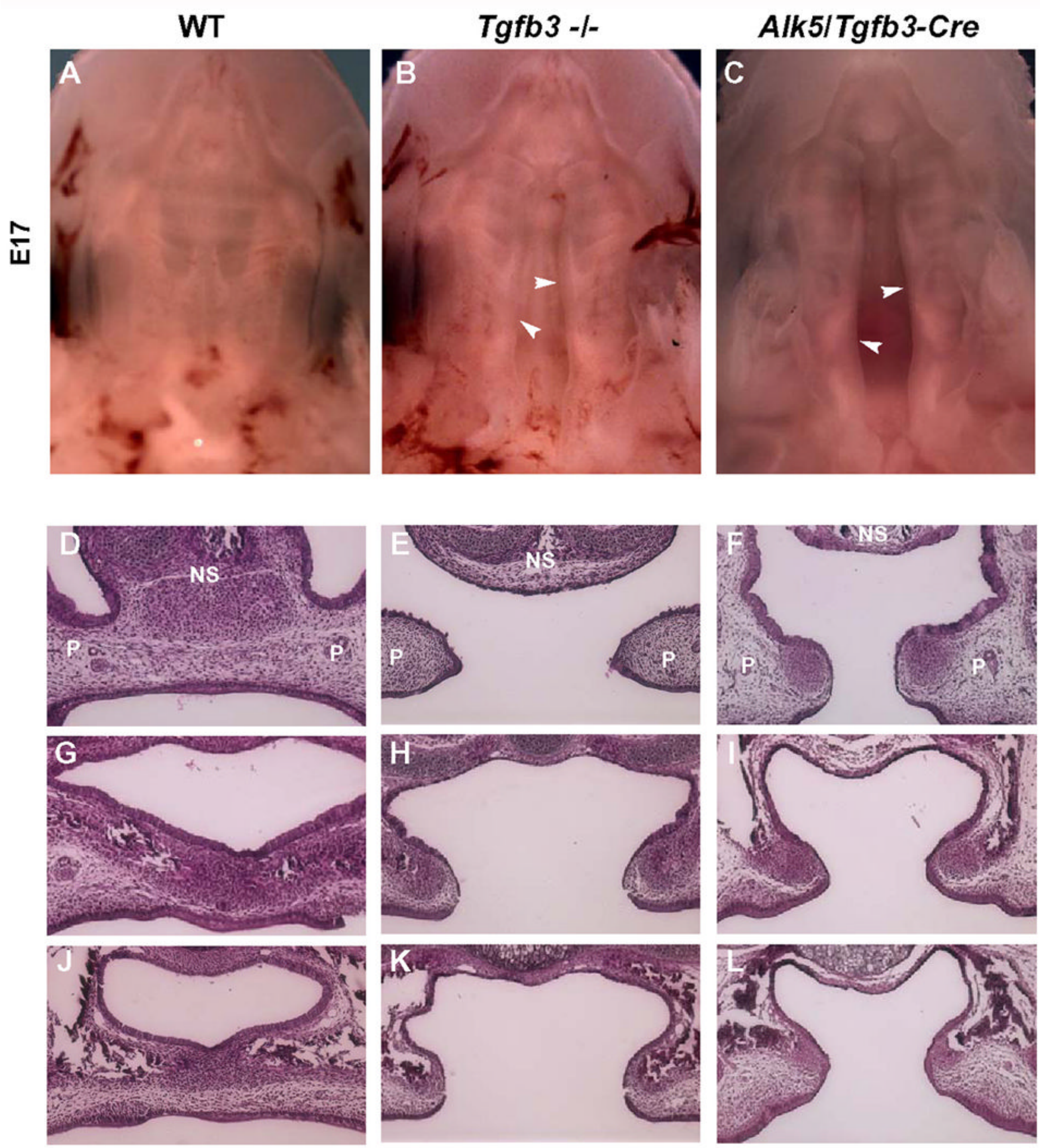

FIG. 4.

Tgfb3-Cre driven abrogation of the TGF-β type I receptor Alk5 leads to a palatal phenotype identical to that seen in Tgfb3 null mice. Stereoscopic images of the formalin-fixed E17 heads from wildtype (a), *Tgfb3*−/− (b), and *Alk5/Tgfb3-Cre* (c) embryos after removal of the mandible. (d–l) Selected frontal sections along the anterior–posterior axis from wild-type (d,g,j), *Tgfb3*−/− (e,h,k), and *Alk5/Tgfb3-Cre* (f,i,l) embryos. Cleft palate phenotypes of *Tgfb3* −/− and *Alk5/Tgfb3-Cre* samples are identical.

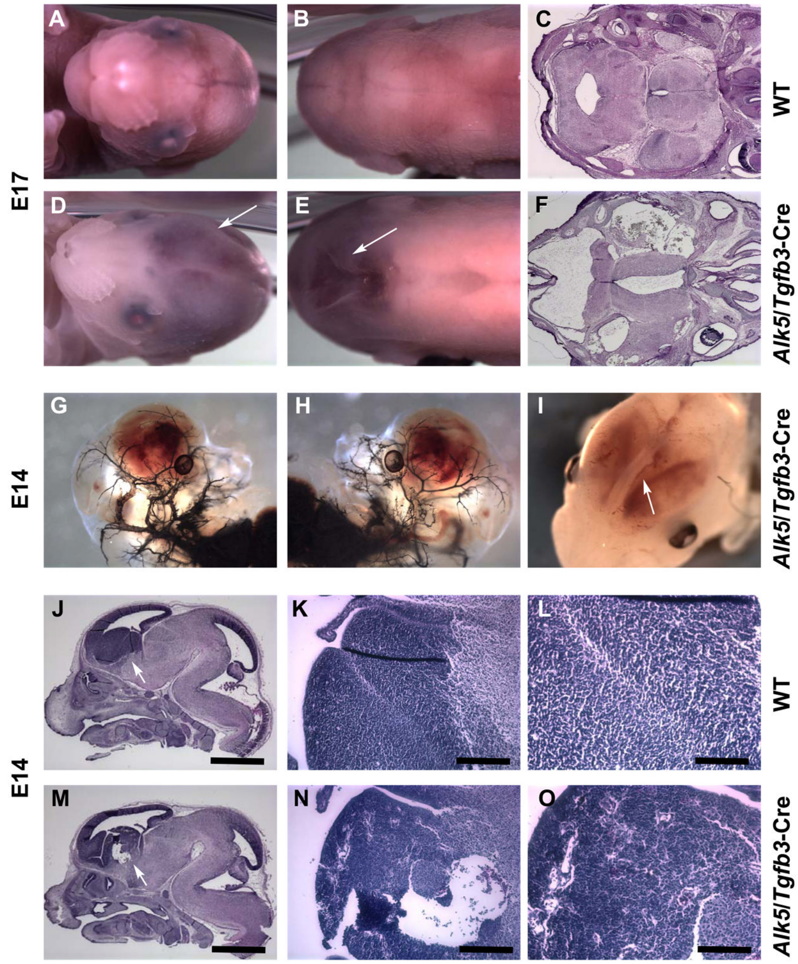

FIG. 5.

Analysis of the intracranial hemorrhage phenotype resulting from *Tgfb3-Cre* driven abrogation of the TGF-β type I receptor Alk5. (a–f) Stereoscopic and histological images of the control (a–c) and *Alk5/Tgfb3-Cre* mutant samples (d–f) at E17. *Alk5/Tgfb3-Cre* mice displayed intracranial hemorrhage (d, arrow) and tissue collapse at the hindbrain region (e, arrow). Coronal sections of the head revealed that the mutant mice have hydrocephalus with dilation of all the ventricles (e). (g,h) Staining of the major arteries of the *Alk5/Tgfb3-Cre* mutant brain by injection of the Indian ink to the left cardiac ventricle (g, right lateral image; H, left lateral image). (i) Stereoscopic image of the intra-cranial hemorrhage of the *Alk5/Tgfb3-Cre* mutant at E14. Note a blood clot (arrow) was trapped in the region surrounding the venous sinuses, the absorption area of the cerebrospinal fluid. (j–o) Sagittal sections of the head of the control (j,k,l) and mutant (l,m,o) embryos at E14 stained with hematoxylin and eosin. The mutant head displayed a hemorrhage in the germinal matrix (arrow) and a rupture through the ependymal cell layer of the ventricle. Selected regions in (j) and (m) (indicated by an arrow) are shown in (k) and (l), and (n) and (o), respectively. Scale bars, 1 mm in (j) and (m); 250 lm in (k) and (n), and 125 lm in (l) and (o).